

# Oscillating flow in a parallel-plate stack of a standing wave thermoacoustic resonator: PIV measurements within the entrance region

Xiaoan Mao, Zhibin Yu, Artur J. Jaworski<sup>(✉)</sup>

The University of Manchester, School of Mechanical Aerospace and Civil Engineering, Manchester, UK, a.jaworski@manchester.ac.uk

**Abstract:** In thermoacoustic devices, an acoustic wave interacts with stacks and heat exchangers in a resonator. Placing such internal structures, in what is essentially an oscillatory flow, produces complex flow phenomena around their extremities due to the introduction of cross-sectional discontinuities. One of the simplest geometries of stacks and heat exchangers can be imagined as a series of parallel plates; velocity profiles in the channels in between are disturbed by the entrance effects.

In this work, particle image velocimetry (PIV) is used to investigate the flow structure in the “entrance region”. Velocity profiles of the oscillating air flow within the channel of a parallel-plate stack, placed in a standing wave resonator, were measured as a function of phase and distance from the stack end. Using the data obtained, this work attempts to quantify an “entrance length” (by analogy with existing fluid mechanical definitions). Its estimations are carried out over the half cycle of an oscillation period, when the working gas is known to flow into the stack. This is followed by the discussion of future uses of the methodology presented.

**Key words:** Entrance region, standing wave, stack, thermoacoustic.

## A. Introduction

The linear thermoacoustic theory, based on Rott’s acoustic approximation [1], [2] is one of the most popular tools of thermoacoustic analysis. However, it is known that “entrance effects”, caused by discontinuities of the cross-sectional area, such as stacks, regenerators and heat exchangers, affect the behaviour of the oscillatory flow, and are difficult to account for within the linear thermoacoustic theory, particularly if the flow physics is not well understood. Furthermore, as the drive ratio is continually increased beyond the validity of the linear approximation, the combination of the “entrance effects” and the “turbulent transition” (e.g. the occurrence of turbulent bursts within the cycle) makes the modelling even more challenging. The work presented here is a continuation of similar studies, which were conducted earlier, of fluid behaviour close to the geometrical discontinuities, e.g. [3], [4], but looks specifically at the definitions of “entrance lengths” in the context of thermoacoustic flows, using both the experimental data obtained from PIV and CFD simulations.

The concept of “entrance length”,  $l$ , is well understood for steady flows. It can be defined for

example, as the distance from the channel entry to the point where the centreline velocity deviates 1% from the fully developed value [5], [6]:

$$u(l,0) - u(\infty,0) = 0.01u(\infty,0). \quad (1)$$

However, such definition cannot be easily used for unsteady (time-dependent) flows. Atabek & Chang [5] and Krijger [6] studied a class of problems referred to as “pulsatile” flows where an oscillatory flow is superimposed onto a steady component. It was postulated that the “entrance length” must be defined as a function of time (or phase) as follows:

$$u(l(t),0,t) - u(\infty,0,t) = 0.01nu_{ref} \quad (2)$$

where  $n$  is a “tolerance number” and  $u_{ref}$  is an appropriately chosen reference velocity. Atabek & Chang [5] suggested that  $u_{ref}$  should be the steady component of velocity, but this leads to ambiguities in purely oscillating flows occurring in thermoacoustic applications, where the amplitude of the velocity oscillation is a more convenient choice. Gerrard and Hughes [7] carried out flow visualisations based on pH indicators and using cine-film photography to validate findings of [5] and [6], and proposed a correlation for the entrance length from the velocity along the centreline.

Yamanaka et al. [8] studied purely oscillatory flows, and in particular the “entrance length”, using ultrasonic velocity profile (UVP) techniques. In their approach, the Fast Fourier Transform (FFT) analysis of the unsteady velocity at the pipe centreline was carried out and the “entrance length” was identified as the distance from the entrance where the third harmonic becomes negligible.

More recently, the “entrance length” effects were considered in the context of so-called synthetic jets [9], where an oscillatory flow within a small orifice is induced by a flexible oscillating membrane at the bottom of a cavity located underneath. The numerical study conducted by the authors showed that the entrance length is the function of phase angle and that for each phase it could be defined by analogy to equation (2).

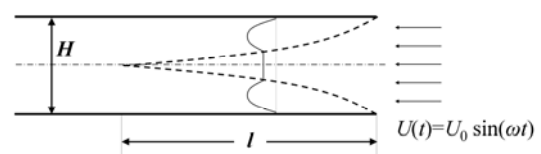


**Fig.1.** Schematic “entrance region” for oscillating flows.

The current work aims at extending these concepts of “entrance length” for oscillatory flows occurring in thermoacoustics. The flow field in a selected channel of the stack is measured using phase-locked PIV, close to the stack extremity. The “entrance length” is estimated over the half cycle of an oscillation period, when the working gas is known to flow into the stack, using the instantaneous values of velocity on the channel centreline.

## B. Experimental apparatus and method

The experimental apparatus (Figure 2) is described in detail in [10]. The resonator consists of a 7.4 m long square duct, with internal dimensions 136x136 mm, and a cubical box coupled via a 300 mm long contraction. The acoustic excitation is provided by a 600 W woofer (PD1850), mounted on the box, and fed with a sine wave from a TTI TG1010A function generator, amplified by a power amplifier. In the  $\frac{1}{4}$ -wavelength mode, the rig works at 13.1 Hz. The opposite end of the resonator has an end-plate with a flush-mounted pressure transducer (Endevco 8510B-2) to measure the drive ratio and to serve as a reference for phase-locking of PIV. The working gas is air at atmospheric pressure and room temperature.

The stack used in this work is made of eight 5.0 mm thick, 200 mm long ( $L$ ), evenly-spaced Perspex plates, forming channels of height (width)  $H = 10.0$  mm. The stack is placed 4.1 m ( $0.16\lambda$ ) from the end plate.

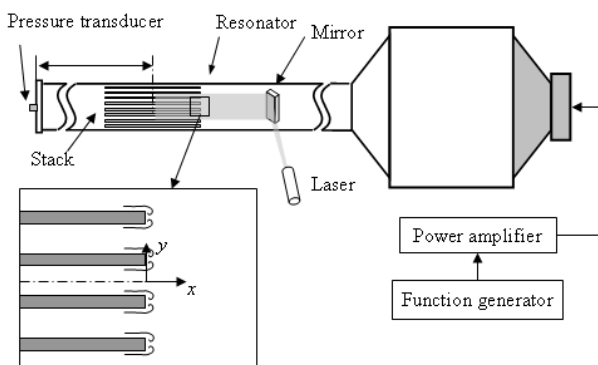


**Fig.2.** Schematic drawing of the thermoacoustic device and the investigated region in the stack of plates.

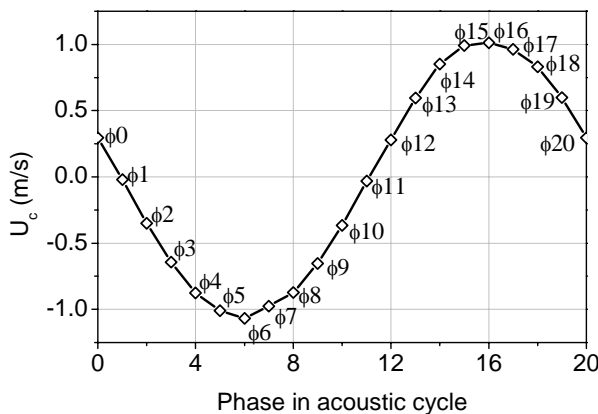


**Fig.3.** Phase points used in PIV phase locked measurement corresponding to the acoustic cycle.

The flow is seeded with the mist of glycerol and water mixture, with the particle size around 5~15  $\mu\text{m}$ . A plane parallel to the rig’s length, but perpendicular to the stack’s plates is illuminated by a laser sheet from a Big Sky twin-head pulsed laser, using a mirror mounted inside the resonator, 900 mm away from the centre of the stack to minimise the flow disturbance. A CCD camera (TSI Powerview Plus 4MP) with a pixel array of 2048 x 2048 is used to capture the images. A synchronizer controls the timing between the laser flashing and image capturing. The synchronizer is triggered externally by a TTL signal generator, which uses the output of the pressure transducer mounted at the end of the resonator as a phase reference. Therefore, PIV images can be phase-locked to the pressure oscillation in the standing wave resonator. In general, 100 pairs of images are taken for each phase to obtain ensemble-averaged velocity and vorticity fields. The images are processed with a commercial package (TSI Insight 3.3) using cross-correlation technique. 32 x 32 interrogation areas are used with 50% overlap. The spatial resolution of measured velocity field achieved is about 0.15 mm. The area interrogated by PIV is shown schematically in Figure 2. It is around 31x31 mm, with the plate end located at the centre. The flow is typically studied at 20 selected phases within the acoustic cycle (Figure 3).

## C. Experimental results and discussion

The experimental results discussed here are taken for the drive ratio,  $D_r = 0.3\%$ . The corresponding velocity amplitude within the stack channel,  $u_a$ , is 0.95 m/s. The oscillatory Reynolds number based on the viscous penetration depth  $\delta_v = (2\nu/\omega)^{1/2}$  and  $u_a$ ,  $Re_\delta = 2^{1/2} u_a \delta_v / \nu$ , is around 50, much lower than the critical value of 400 found by Merkli and Thomann [11]. Therefore the flow is likely to remain laminar inside the channel.

Figure 4 shows typical results for two selected phases (3 and 6). The colour map shows the vorticity field of the flow around the entrance, while the velocity is depicted by black arrows. In phase 3, a pair of vortices formed at the corners of the plates, together with weaker vortex structures that had been formed in the “ejection phase” earlier, are swept inside the channel (phase 6) [4]. The system of counter-rotating vortices causes the retardation of axial velocity in the channel centre, and an overshoot of the axial velocity near the walls as shown in the velocity profiles presented in Figure 5, discussed below.

Figure 5(a-c) shows a series of axial velocity profiles extracted from PIV data, plotted as a function of the normalised distance from the channel inlet,  $x/\xi_a$ , where  $\xi_a$  is the displacement amplitude within the channel (11.6 mm for  $D_r = 0.3\%$ ) for three arbitrarily selected phases: 2, 3 and 6, respectively. Because of the coordinate system defined in Figure 2, the normalised distance is negative in the direction “into the channel”. The velocity profiles for individual axial locations are shifted in the graphs to their corresponding distance from the plate end, which can be read at the  $2y/H = \pm 1.0$  for each profile.

As suggested for example in [8] and [9], in order to estimate the “entrance length” one would have to look at

the velocity profiles, such as presented in Figure 5, on the phase-by-phase basis and evaluate the location at which the profiles do not differ significantly from one another. For example, looking at Figure 5a, one would estimate that for phase 2 the velocity profiles stop changing after reaching  $x/\xi_a$  of around -0.5, but for phase 6, such an “entrance length” would extend somewhere beyond  $x/\xi_a=-2$ .

However, looking at PIV images and the resulting velocity profiles is cumbersome. Ideally one would like to develop simpler methods of judging the extent of the “entrance length”. Therefore, as one possible method, it is proposed to look at the ratio of the velocity on the channel centreline,  $u_c$ , to the velocity amplitude,  $u_a$ . The corresponding charts d-f in Figure 5 show the absolute value of such a ratio. It is relatively easy to see that the “entrance length” would be about 0.4, 0.8 and more than 2 of  $x/\xi_a$ , for phases 2, 3 and 6, respectively. In graphs d-f, circles denote experimental results, while the solid lines are obtained from numerical simulations as explained below.

To aid the analysis of the “entrance region”, which is

clearly affected by the transport of vorticity into the channel, a CFD model has been set up for the conditions corresponding to the experiment in order to predict the flow around the end of the stack. The model was set up in FLUENT 6.2 and the large eddy simulation (LES) model was chosen for turbulence prediction. A pseudo-three-dimensional geometry was set up with only one mesh element in the direction perpendicular to the main flow. The structured mesh includes 146,000 nodes. The second order implicit scheme was used for time integration. The time step is 1/80 of the oscillation period. SIMPLE scheme is used for pressure velocity coupling. As mentioned above, the numerical velocity distributions along the channel centreline for the three chosen phases are plotted as solid lines in Figure 5(d-f). It can be seen that the numerical results are in a very good agreement with the experimental results, although for phase 6 there are some small discrepancies. Nevertheless the simulation seems to predict correctly the position of the vortex structures, causing the “dip” in the profile in Figure 5f, around  $x/\xi_a=1.0$ .

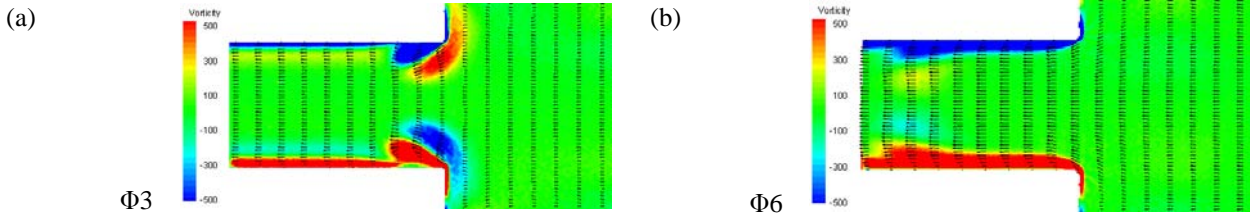


**Fig.4.** Ensemble-averaged axial velocity and vorticity fields at the entrance to the channel in a parallel-plate stack. Axial component of the velocity is shown by the black arrows, while the vorticity (in 1/s) is shown using a colour scale. Phases 3 and 6 are shown.

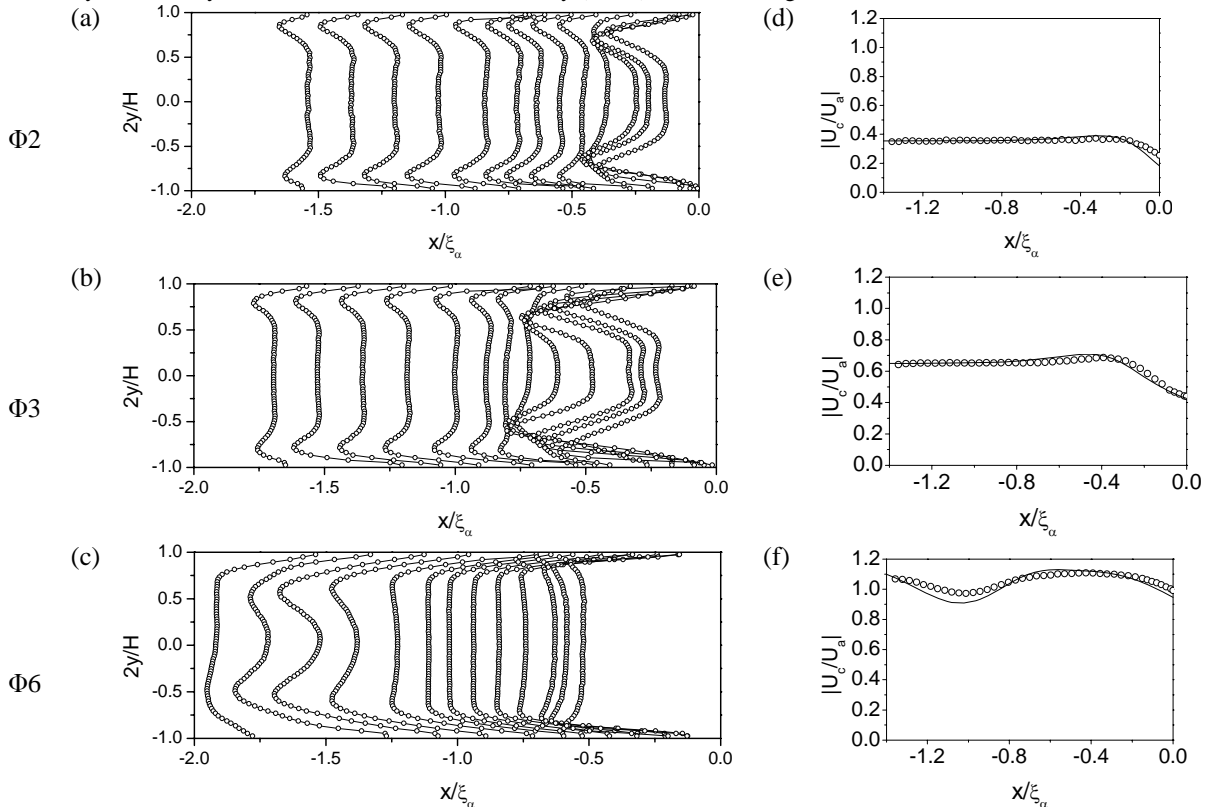


**Fig.5.** Flow velocity in the channel. (a-c) Axial velocity profile in the cross sections of different distances away from the channel entrance. (d-f) Axial velocity distribution along the channel centreline (Circles – experiments, solid line – CFD). Three phases: 2, 3 and 6 are shown.

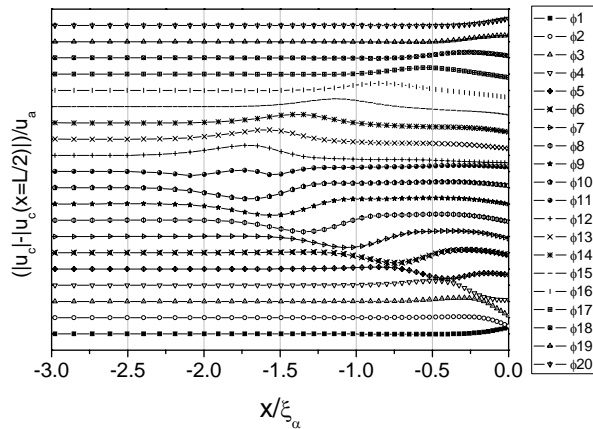


**Fig.6.** Axial velocity in the channel centre line in twenty phases.

Figure 6 shows the results obtained from the numerical simulations for the corresponding 20 phases. Here, for the clarity of the graph, the ratio  $|u_c/u_a|$  was replaced by the difference between the velocity on the centreline for a given  $x/\xi_a$  and the velocity on the centreline in the middle of the stack ( $x/\xi_a \approx -9$ ) normalised by the velocity amplitude. The “wavy pattern” reveals the extent of the “entrance length” phase-by-phase. It can be seen that the “entrance region” extends the furthest into the channel for phase 11 and that the “entrance length” in this case is about  $2.5\xi_a$ .

#### D. Conclusions and future work

This paper presents a preliminary study of the entrance effects in the oscillatory flows within the parallel-plate stack of a standing-wave thermoacoustic system. PIV is used to obtain the time-dependent velocity profiles within the channel. This data is further used to investigate the distance referred to as the “entrance length”. It is suggested that in order to obtain the “entrance length”, the velocity information could be significantly reduced to include only the values at the channel centre-line. Two such “data reduction” techniques were illustrated, to include  $|u_c/u_a|$  and  $(|u_c| - |u_c(x=L/2)|)/u_a$  characteristics as a function of  $x/\xi_a$ .

The significance of this work is twofold. Firstly, it should be recognised that conducting PIV measurements is usually non-trivial, and for most realistic thermoacoustic systems it is usually not straightforward. Therefore, establishing the “entrance lengths” from more limited data sets than the full velocity/vorticity field may be advantageous for researchers trying to establish the influence of geometrical discontinuities in their thermoacoustic systems. For example, the use of a limited amount of hot-wire measurements may prove equally effective as the use of PIV. Secondly, from a fundamental perspective, thermoacoustic flows are not identical to the cases described in the existing literature reviewed in the introduction. In particular, it is clear that the velocity profile at the entry to the channel is never flat, as is the case for piston-induced pipe flows [7], [8].

Therefore it is likely that thermoacoustic flows will require different correlations to predict “entrance lengths”. The methodology described in this paper is the first step in this direction.

However it is recognised that the work presented focuses only on one (small) drive ratio in a fixed geometrical configuration. In order to generalise the findings, one needs to consider the whole range of drive ratios, together with variable geometrical ratios, such as, for example, the ratio of plate thickness to the channel width or plate thickness to acoustic displacement. Further work will focus on the mixture of experimental and numerical approaches to devise appropriate general correlations for the “entrance length” in thermoacoustic systems. It is hoped that this information will help development of thermoacoustic models such as DELTAE, or its equivalents.

#### E. Acknowledgements

The support received from EPSRC (UK) is gratefully acknowledged. The authors would also like to thank Mr Xuerui Mao for his help in CFD modelling.

#### F. Literature

- [1] N. Rott, "Thermoacoustics" Adv. Appl. Mech., vol. 20, pp. 135, 1980.
- [2] G. W. Swift, "Thermoacoustics: A Unifying Perspective for some Engines and Refrigerators" Acoustical Society of America, New York, 2002.
- [3] P. Blanc-Benon, E. Besnoin and O. Knio, "Experimental and computational visualization of the flow field in a thermoacoustic stack". C. R. Mecanique, vol. 331, p. 17-24, 2003.
- [4] X. Mao, D. Marx and A. J. Jaworski, "Measurement of Coherent Structures and Turbulence Created by an Oscillating Flow at the End of a Thermoacoustic Stack", Proc. iTi Conference in Turbulence, 25-28 September 2005, Bad Zwischenahn, Germany; to be published in vol. 109 of "Springer Proceedings in Physics" series, 2007
- [5] H. B. Atabek and C. C. Chang, "Oscillating flow near the entry of a circular tube" Z. Angew. Math. Phys., vol. 12, pp. 185, 1961.
- [6] J. K. B. Krijger, B. Hillen, H. W. Hoogstraten, "Pulsate entry-flow in a plane channel" Journal of Applied Mathematics and Physics (ZAMP), vol. 42, pp. 139, 1991
- [7] J. Gerrard. and M. Hughes, "The flow due to an oscillating piston in a cylinder tube: a comparison between experiment and a simple entrance flow theory" J. Fluid Mech., vol. 50, pp. 97, 1971.
- [8] G. Yamanaka., H. Kikura, Y. Takeda, M. Artomi, "Flow measurement on an oscillating pipe flow near the entrance using the UVP method" Exp. in Fluids, vol. 32, pp. 212, 2002
- [9] R. Raju, R. Mittal, Q. Gallas, L. Cattafesta "Scaling of velocity flux and entrance length effects in non-net mass flux devices" AIAA-2005, pp. 4751, 2005
- [10] D. Marx, X. Mao, A. J. Jaworski, "Acoustic coupling between the loudspeaker and the resonator in a standing wave thermoacoustic device", Applied Acoustics, vol. 67, pp. 402, 2006
- [11] P Merkli and H Thomann, "Thermoacoustic effect in resonance tube", J. Fluid Mech., vol. 70, pp. 161-177, 1975.